Journal of Dynamical Systems and Complexity (2025) **1**(1), 20-28

On The Synchronization Of Memristive Neural Networks

Eduardo Elpidio Rodríguez Martinez [*], José de Jesús Esquivel Gómez
and Juan Gonzalo Barajas Ramírez

División de Control y Sistemas Dinámicos, Instituto Potosino de Investigación Científica y Tecnológica A.C., San Luis Potosí, Mexico

Abstract

Neural systems consist of neurons connected by synapses that can be modeled as circuits to represent their electrical behavior. In particular, when memristors are used to capture features of biological neurons or synapses, the resulting model is called a memristive neural network (MNN). In this contribution, we propose a class of MNN, based on Hindmarsh–Rose (HR) neuron models coupled by memristors as synapses with parameters chosen to produce typical responses of chemical synapses. We show that identical synchronization in this class of MNN is achieved for a sufficiently large coupling strength, while the features of passive memristors as chemical synapses affect the emergence of synchronization. Our results are illustrated with numerical simulations.

Keywords— Neuron models, Synchronization, Memristive Synapses

1 Introduction

Computational intelligence has its origins in the attempts to model the way information is processed in biological neural systems. To model the brain's capacity to process information, one starts with neurons as the basic processing units, which are then coupled into large ensembles by special connections called synapses, where different aspects of the structure and communication result in highly complex patterns of behavior, like classification, memory and learning. The basic framework to model the physiological behavior of neurons and synapses is an electrical circuit with voltage-dependent conductance to describe the effects of ionic densities that induce currents in the neuron's membrane and within the synaptic gap [1].

A model of the brain's processing capacity is based on neurons acting as primary processing units and interconnecting them through special connections known as synapses to create large ensembles that result in extremely complex patterns of behavior, including classification, memory, and learning, as a result of different aspects of the structure and communication.

The main behavior associated with neurons is the nonlinear feature of excitability, which means that small external inputs have almost no response; however, a larger stimulus moves the neuron's electrical activity far from the quiescent state and results in a large excursion of current away from its resting state, followed by a refractory period that separates one reaction from the next. This phenomenon in neuroscience is known as an action potential. Synapses are the extracellular spaces where transmission of the action potentials between presynaptic and postsynaptic neurons takes place. The neural communication is modeled as an electrical-chemical phenomenon produced by the movement of ionic charges through channels in neuron's membrane. The ionic currents that move via gap junctions are the electrical part of the synapses, this part is usually represented with a fixed bidirectional conductivity. On the other hand, the ionic currents due to changes in the concentration of neurotransmitter are the chemical synapses, which are modeled by a time-varying directed conductivity that is dependent on the voltage difference in the synaptic gap. In this way, the efficiency of transmission becomes adjustable due to accumulation of action potential that excite or inhibit other neurons in the network. This phenomenon in neuroscience is called plasticity, an important feature of complex neural behaviors [2, 3].

The most direct interpretation of the physiological features discussed above is the McCullogh-Pitts model, in it neurons are defined as accumulators of binary inputs and biases, that produce an output due to an activation function. Then, a neural network is formed by layers of neurons that are connected via fixed synaptic weights which are adjusted to approximate an unknown function that correctly assigns inputs to outputs. Determining the best values for the synaptic weights from experimental data in the form of training and validating sets, is called

---

[*] Corresponding author: eduardo.rodriguez@ipicyt.edu.mx

machine learning (ML). In general, realizations of this model are called Artificial Neural Networks (ANN), while their computational applications are usually called Artificial Intelligence (AI) [4].

In recent years there has been a growing interest in the construction of engineering systems that process information in a way that more closely resembles the biological reality. These efforts for a more neuromorphic models and realizations are made in hope that complementing the ANN model with the objective to improve its performance or providing it with additional features that can be realized in computational intelligence. In these sense, an encouraging approach is the use of memristors in neural models [5]. Although some years have past since the initial use of memristors in models of neuroscience it can be argued that this area of research is still at an early stage, with basic questions like the emergence of synchrony between memristive neural models remaining a significant open problem.

Memristors are theoretical two-terminal devices that obey an Ohm's law dependent on internal variables. That is, the resistive part of the current-voltage relation changes according to the evolution of internal variables and the input to the device, effectively becoming a resistive memory when the vector field becomes null [6].

There are different versions of memristor in the literature, the original proposal of Chua, also known as the ideal memristor, was conceived as the fourth basic electronic component, which relates electric charge to magnetic flux, taking the time derivative, results in a current to voltage relation given by as a function of magnetic flux or electric charge as its internal variable [7]. This theoretical device was associated with a semiconductor nano-material with Titanium dioxide doping called the HP-memristor [6]. However, as doped area is not the same as magnetic flux, this is an extension of the ideal memristor, usually called a memresistive system [8]. Taking this approach many different electronic systems can be expressed as memristors. In particular, the characteristics of memristors are useful to describe electro-chemical features of biological neural systems. Namely, the voltage dependent conductance of the neuron's membrane and the synaptic connection can be directly modeled as memristive systems where the concentrations of ionic charges are the internal variables [9].

In this contribution, we consider a class of neural network, where the neurons are modeled as oscillator capable of generating bursts of action potentials, while their coupling synapses are memristors that aim at reproducing the features of chemical synapses. For this memristive neural network (MNN) we are interested in determining conditions under which the bursting behavior of the neurons become synchronized and the effect of synaptic weight on the stability of this synchronized behavior.

The remainder of the paper is organized as follows. On Section II, the MNN model is presented with detail. In Section III, the main result of this contribution is presented as a condition on the coupling weight of the memristor synapses. Numerical simulations to illustrate our results are shown in Section IV, then in closing, some comments and remarks are given in Section V.

2 A Memristive Neural Network Model

Consider a network where each node is a Hindmarsh-Rose (HR) neuron of the form [10]:

$$\begin{bmatrix} \dot{x}_1(t) \\ \dot{x}_2(t) \\ \dot{x}_3(t) \end{bmatrix} = \begin{bmatrix} x_2(t) - x_1(t)^3 + bx_1(t)^2 - x_3(t) + I(t) + I_{syn}(t) \\ 1 - dx_1(t)^2 - x_2(t) \\ r(s(x_1(t) - x_o) - x_3(t)) \end{bmatrix} \tag{1}$$

where $x_1(t)$ is the neuron's membrane voltage, $x_2(t)$ is the recovery and $x_3(t)$ is the adaptation variable. The variables $x_1(t)$ and $x_2(t)$ constitute the fast subsystem, while $x_3(t)$ is the slow subsystem. In this model, $I(t)$ is an external input current, b is a parameter that control the spiking frequency and it allows to change the neuron dynamics from bursting to spiking; the slow activation of the current $x_3(t)$ is modulated through the small parameter $0 < r << 1$, which is treated as a rate of current activation; while x_o is a control parameter that activate or eliminate activation of the slow current. A typical choice of parameter values for (1) is $b = 2.7$, $d = 5$, $s = 4$, $x_o = -1.6$ and $r = 0.006$ with $I(t) = 4$, results in the square-wave bursting behavior shown in Figure 1.

The neurons are coupled by synaptic currents ($I_{syn}(t) = I^E_{syn}(t) + I^C_{syn}(t)$) with the electric part:

$$I^E_{syn}(t) = g_e[V_i(t) - V_j(t)] \tag{2}$$

which is dependent on the voltage difference between pre ($V_i(t)$) and postsynaptic ($V_j(t)$) neurons with a constant conductance g_e. The chemical part is given by:

$$I^C_{syn}(t) = g_c[V_i(t) - V_s]\Gamma(V_i(t)) \tag{3}$$

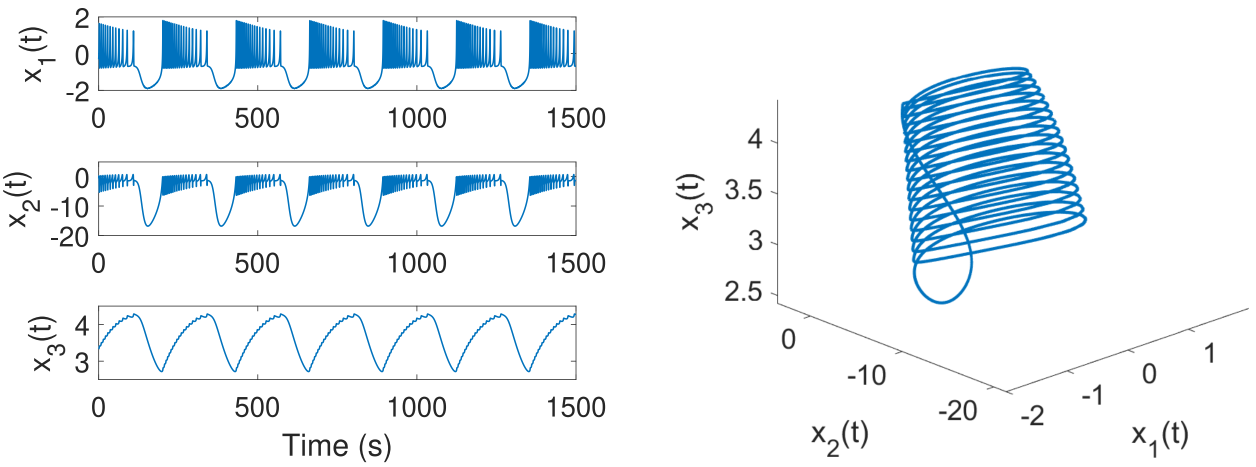

Figure 1: Dynamical behavior of the HR neuron model (1) and initial condition $(-0.3079, -0.5729, 3.3288)$.

where g_c is a constant conductance and depending on the bias voltage V_s the resulting current can be excitatory (positive) or inhibitory (negative). $\Gamma(\cdot)$ is a nonlinear function that represent the saturation behavior of the neurotransmitter and ionic concentrations on the synaptic gap, which is usually approximated as a sigmoid function of the form:

$$\Gamma(V_i(t)) = \frac{1}{1 + exp^{-\lambda(V_i(t)-\Theta_s)}} \tag{4}$$

where λ and Θ_s are constants use to adjust speed and cutoff of the saturation function (see Figure 2).

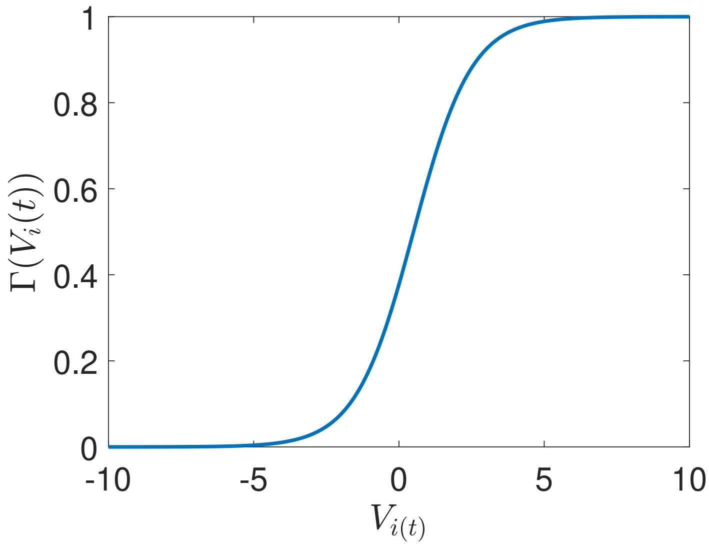

Figure 2: Visualization of the saturation function $\Gamma(V_i(t))$, a sigmoidal approximation used to model the nonlinear relationship between membrane voltage and synaptic behavior. The plot highlights how $\Gamma(V_i(t))$ transitions smoothly from 0 to 1, with its slope and threshold controlled by λ and Θ_s, respectively. This function is essential for simulating the bounded response of synaptic currents, ensuring biological plausibility in Eq. (3).

On the other hand, the properties of memristors can be used to characterize biological neural systems. These devices are described by two equations:

1. An algebraic relation that describes the current-voltage relationship in terms of a variable dependent Ohm law

$$\mathcal{I}(t) = W(\phi(t))\mathcal{V}(t) \tag{5}$$

where $W(\cdot)$ is the memductance function.

2. A differential equation
$$\dot{\phi}(t) = f(\phi(t), \mathcal{V}(t)) \tag{6}$$
where $f(\cdot)$ describes the dynamical evolution of the internal variable ($\phi(t)$) with a voltage input ($\mathcal{V}(t)$).

An important feature of memristors is that its resistive value ($W(\phi(t))$) depends on the history of the input applied to the device, furthermore, in the case when $f(\phi(t), \mathcal{V}(t)) = 0$, $\phi(t)$ becomes a constant, *i.e.* a nonvolatile resistive memory. Additionally, if the resistance $W(\phi(t))$ is strictly positive for any value of $\phi(t)$, the device is passive, *i.e.* it only consumes energy [6]. In this representation, if $f(\phi(t), \mathcal{V}(t)) = \mathcal{V}(t)$, one obtains an ideal memristor, which has resistive nonvolatile memory and it is passive [7].

Using the memristor (5)-(6) to describe the chemical synapses that connects two HR neurons, many different options can be considered. Perhaps the most direct approach is to have an ideal memristor of the voltage difference between neurons with a memductance that approaches a sigmoid function. This approximation captures two relevant features of biological chemical synapses: (i) the saturation of the synaptic response at large voltages (the amount of neurotransmitter and the channel opening have a physical limit), and (ii) the smooth transition between inactive and active states, reflecting the continuous dependence of neurotransmitter release on the presynaptic potential. The sigmoid also provides numerical and analytical advantages, which facilitates theoretical demostration and numerical integration. This choice is not exclusive, functions such as piecewise linear or trigonometric functions like $\tanh(\phi(t))$ to approximate (4) [11] can be used with similar criteria.

In this contribution, we consider that the synaptic current that connects two HR neurons (1) is both electric and chemical, that is, it has an electric part
$$I_{ij}^{E}(t) = g_e[u_{ij}(t)] \tag{7}$$
and a chemical part represented as a memristive synapse
$$\begin{cases} I_{ij}^{C}(t) &= g_c[u_{ij}(t) - v_s]\Gamma(\phi_{ij}(t)) \\ \dot{\phi}_{ij}(t) &= u_{ij}(t) \end{cases} \tag{8}$$
where $u_{ij}(t) = x_{i1}(t) - x_{j1}(t)$ denotes the membrane potential difference between neuron i and neuron j, and $\Gamma(\phi_{ij}(t)) = 1/[1 + \exp^{-\lambda(\phi_{ij}(t) - \Theta_s)}]$ as the memductance function. Conventional values for the chemical coupling of HR neurons are $\lambda = 10$ and $\Theta_s = -0.25$ with $v_s = 2.0$ for excitatory and $v_s = -2.0$ for inhibitory effects [12].

In our analysis and simulations, the chemical synapses are thus modeled as an ideal memristor (8). The sigmoidal memductance $\Gamma(\phi_{ij}(t))$ ensures $W(\phi_{ij}) > 0$ for all ϕ_{ij}, thereby satisfying the passivity condition. Moreover, since $\phi_{ij}(t)$ integrates $u_{ij}(t)$, it converges to a constant when $u_{ij}(t) \to 0$, preserving the memory effect of the memristive synapse.

Using the above descriptions, the dynamic of a HR neurons in a network connected via memristive synapses is given by

$$\begin{bmatrix} \dot{x}_{i1}(t) \\ \\ \dot{x}_{i2}(t) \\ \\ \dot{x}_{i3}(t) \end{bmatrix} = \begin{bmatrix} x_{i2}(t) - x_{i1}(t)^3 + bx_{i1}(t)^2 - x_{i3}(t) + I + g_e \sum\limits_{j=1, j\neq i}^{N} a_{ij}[u_{ij}(t)] + g_c \sum\limits_{j=1, j\neq i}^{N} b_{ij}[u_{ij}(t) - v_s]\Gamma(\phi_{ij}(t)) \\ \\ 1 - dx_{i1}(t)^2 - x_{i2}(t) \\ \\ r(s(x_{i1}(t) - x_0) - x_{i3}(t)) \end{bmatrix} \tag{9}$$

$$\dot{\phi}_{lk}(t) = b_{lk}u_{lk}(t) \tag{10}$$

for $i, l, k = 1, 2, ..., N$ where g_e and g_c are uniform strength of connections for electrical and chemical connections, respectively. The structure of the network is given by the matrices $A = \{a_{ij}\} \in \mathbf{R}^{N\times N}$ and $B = \{b_{ij}\} \in \mathbf{R}^{N\times N}$. In both cases, if the i-th neuron is electrically connected to the j-th neuron with $j \neq i$, then $a_{ij} = a_{ji} = 1$ ($b_{ij} = b_{ji} = 1$); otherwise $a_{ij} = a_{ji} = 0$ ($b_{ij} = b_{ji} = 0$).

If the diagonal elements satisfy the diffusive condition:

$$a_{ii} = -\sum_{j=1, j\neq i}^{N} a_{ij} \text{ and } b_{ii} = -\sum_{j=1, j\neq i}^{N} b_{ij}, \forall i \tag{11}$$

the Laplacian matrices A and B are zero-sum by rows and columns $\sum_{j=1}^{N} a_{ij} = \sum_{j=1}^{N} a_{ji} = 0$, therefore are negative semi-definitive and with zero as an eigenvalue of multiplicity one [13].

The MNN (9)-(10) can be rewritten in vector form as:

$$\begin{aligned} \dot{X}(t) &= \mathbf{F}(X(t)) + \\ &\quad g_e(A \otimes \Lambda)X(t) + \\ &\quad g_c(B \otimes \Lambda)(X(t) - \bar{V})\bar{\Gamma}(\Phi(t)) \end{aligned} \tag{12}$$

$$\dot{\Phi}(t) = \mathbf{B_v} U(t) \tag{13}$$

where $X(t) = [x_1^\top(t), x_2^\top(t), ..., x_N^\top(t)]^\top \in \mathbf{R}^{3N}$, $\mathbf{F}(X(t)) = [F(x_1(t))^\top, F(x_2(t))^\top, ..., F(x_N(t))^\top]^\top \in \mathbf{R}^{3N}$, with $F(x_i(t)) = [F_1(x_i(t)), F_2(x_i(t)), F_3(x_i(t))]^\top = [x_{i2}(t) - x_{i1}(t)^3 + bx_{i1}(t)^2 - x_{i3}(t) + I, 1 - dx_{i1}(t)^2 - x_{i2}(t), r(s(x_{i1}(t) - x_o) - x_{i3}(t))]^\top$, $\Lambda = diag([1,0,0]) \in \mathbf{R}^3$ and $\bar{V} = [V_s^\top, ..., V_s^\top]^\top = [[v_s, 0, 0]^\top, ..., [v_s, 0, 0]^\top]^\top \in \mathbf{R}^{3N}$. While the internal variables of the memristors are $\Phi(t) \in \mathbf{R}^{N^2}$, with the matrix $\mathbf{B_v} = diag([A(:,1), A(:,2), ..., A(:,N)]) \in \mathbf{R}^{N^2 \times N^2}$, and $U(t) = [u_{11}(t), ..., u_{1N}(t), ..., u_{N1}(t), ..., u_{NN}(t)]^\top \in \mathbf{R}^{N^2}$.

In the following Section we solve the problem of synchronization for this type of MNN.

3 Synchronization in a class of MNN

One behavior of interest in the MNN is the identical synchronization between neurons. In particular, asymptotic synchronization, which means that the solution of (12) to a given initial condition $[X(0), \Phi(0)]^\top \in \mathbf{R}^{3N+N^2}$ satisfy the following conditions:

$$\begin{gathered} x_1(t) = x_2(t) = ... = x_N(t) = s(t), \text{ and} \\ \Phi(t) = \bar{\Phi}, \text{ as } t \to \infty \end{gathered} \tag{14}$$

where $s(t) \in \mathbf{R}^3$ is the synchronized solution of the network (9) and $\bar{\Phi} \in \mathbf{R}^{N^2}$ is a constant vector that results from (10) when $U(t)$ becomes zero.

To establish that synchronization in the sense of (14) one needs to shown that the error variables, $e_i(t) = x_i(t) - s(t) \in \mathbf{R}^3$ for $i = 1, 2, ..., N$ have an asymptotically stable zero equilibrium point [13].

The dynamics of the synchronized solution (14) can be determined from (9)-(10) to be:

$$\begin{gathered} \dot{s}(t) = F(s(t)), \text{ and} \\ \phi_{sk} = \mathcal{C}_k \end{gathered} \tag{15}$$

$$\dot{s}(t) = F(s(t)) \tag{16}$$

Notice that since the chemical synapses are represented by ideal memristors at the synchronized solution $s(t)$, all voltages are identical and $u_{ij} = 0, \forall i, j$. Therefore, each multiplier $\Gamma(\bar{\Phi}_{ij})$ is constant.

From (9) and (14) the dynamics of the errors ($e_i(t) = x_i(t) - s(t)$) are found to be:

$$\begin{aligned} \dot{e}_i(t) &= F(x_i(t)) - F(s(t)) + g_e \sum_{j=1}^{N} a_{ij} \Lambda e_j(t) \\ &+ g_c \sum_{j=1}^{N} b_{ij} \Lambda [e_j(t) - V_s] \Gamma(\phi_{ij}(t)) \end{aligned} \tag{17}$$

for $i = 1, 2, ..., N$. In vector form becomes

$$\begin{aligned} \dot{E}(t) &= \tilde{F}(E(t)) + g_e(A \otimes \Lambda)E(t) + \\ &+ g_c(B \otimes \Lambda)[E(t) - \bar{V}](\Gamma_\phi(t) \otimes \Lambda) \end{aligned} \tag{18}$$

where $\Gamma_\phi(t) = \{\Gamma(\phi_{ij}(t))\}$, and $\otimes$ represents the Kronecker product. Additionally, the internal variables $\phi_{ij}(t)$ evolve according to (13).

A Lyapunov candidate function for (18) is:

$$V(E(t)) = \frac{1}{2} \sum_{j=1}^{N} e_j(t)^\top e_j(t) = E^\top(t) E(t) \tag{19}$$

Taking the time derivative becomes

$$\begin{aligned}\dot{V}(E(t)) &= \tfrac{1}{2}E^{\top}(t)\dot{E}(t) + \dot{E}^{\top}(t)E(t) \\ &= \tfrac{1}{2}E^{\top}(t)\left[\begin{array}{l}\tilde{F}(E(t)) + g_e(A\otimes\Lambda)E(t)+ \\ +g_c(B\otimes\Lambda)[E(t)-\bar{V}](\Gamma_{\phi}(t)\otimes\Lambda)\end{array}\right] \\ &+ \left[\begin{array}{l}\tilde{F}(E(t)) + g_e(A\otimes\Lambda)E(t)+ \\ +g_c(B\otimes\Lambda)[E(t)-\bar{V}](\Gamma_{\phi}(t)\otimes\Lambda)\end{array}\right]^{\top}\tfrac{1}{2}E(t)\end{aligned} \tag{20}$$

For $\dot{V}(\cdot) < 0$ a few considerations are taken. First, the following inequality:

$$E^{\top}(t)\bar{F}(E(t)) \le \gamma E^{\top}(t)E(t) \tag{21}$$

is satisfied for the HR neuron model in (1) for a large enough γ [14]. Then, one has

$$\begin{aligned}\dot{V}(E(t)) &\le \gamma E^{\top}(t)E(t)+ \\ &+\tfrac{1}{2}E^{\top}(t)\left[\begin{array}{l}g_e(A\otimes\Lambda)E(t)+ \\ +g_c(B\otimes\Lambda)[E(t)-\bar{V}](\Gamma_{\phi}(t)\otimes\Lambda)\end{array}\right] \\ &+ \left[\begin{array}{l}g_e(A\otimes\Lambda)E(t)+ \\ +g_c(B\otimes\Lambda)[E(t)-\bar{V}](\Gamma_{\phi}(t)\otimes\Lambda)\end{array}\right]^{\top}\tfrac{1}{2}E(t)\end{aligned} \tag{22}$$

By construction, the Laplacian matrices (A and B) are negative semidefinitive. Using an approach similar to the one used in [13], one finds that the contribution of the electric synapses is bounded by the largest not-zero eigenvalue of the A Laplacian (λ_{2_A}), that is:

$$\begin{aligned}&\dot{V}(E(t)) \le \gamma E^{\top}(t)E(t) - g_e|\lambda_{2_A}|E^{\top}(t)E(t)+ \\ &+\tfrac{1}{2}E^{\top}(t)\left[\ g_c(B\otimes\Lambda)[E(t)-\bar{V}](\Gamma_{\phi}(t)\otimes\Lambda)\ \right] \\ &+\left[\ g_c(B\otimes\Lambda)[E(t)-\bar{V}](\Gamma_{\phi}(t)\otimes\Lambda)\ \right]^{\top}\tfrac{1}{2}E(t)\end{aligned} \tag{23}$$

Regarding the final component, the same reasoning can be used with the additional considerations that $\bar{V}$ is a constant and while $\Gamma(*)$ is nonlinear it is saturated to a constant positive value with the velocity determined by λ in (8). As a result one has

$$\dot{V}(E(t)) \quad \le \quad E^{\top}(t)(\gamma - g_e|\lambda_{2_A}| - g_c(|\lambda_{2_B}| - \bar{V})\Gamma(t))E(t) \tag{24}$$

From the above sketched proof. One has the following results: For a sufficiently large electric coupling ($g_e\lambda_{2_A} >> \gamma$) synchronization is achieved if the chemical coupling is sufficiently small if the coupling is excitatory ($\bar{(V)} > 0$) or for any size of the chemical coupling if the coupling is inhibitory ($\bar{(V)} < 0$).

Based on the Lyapunov inequality in (24), where $|\lambda_{2_A}|$ and $|\lambda_{2_B}|$ are the nonzero eigenvalues of the Laplacian matrices A and B, respectively, and $\Gamma_{\max} = \sup_t \Gamma(\phi_{ij}(t))$ denotes the saturation of the memristive gain. Thus, a sufficient condition for asymptotic synchronization is

$$\gamma - g_e|\lambda_{2_A}| - g_c\left(|\lambda_{2_B}| - \bar{V}\right)\Gamma_{\max} < 0. \tag{25}$$

This expression provides approximate analytical thresholds for the coupling strengths:

$$\begin{aligned}g_e &> \frac{\gamma - g_c(|\lambda_{2_B}| - \bar{V})\Gamma_{\max}}{|\lambda_{2_A}|} \\ g_c &> \frac{\gamma - g_e|\lambda_{2_A}|}{(|\lambda_{2_B}| - \bar{V})\Gamma_{\max}}.\end{aligned} \tag{26}$$

Although conservative, these bounds analytically delimit a region in the (g_e, g_c) plane where synchronization of the memristive neural network is ensured.

4 Results

4.1 Numerical simulations

Consider a network of twenty five nodes connected in a scale-free topology generated by the algorithm proposed by Barabási and Albert [13]. Furthermore, each node is a HR neuron as described by (1) and their connection is given

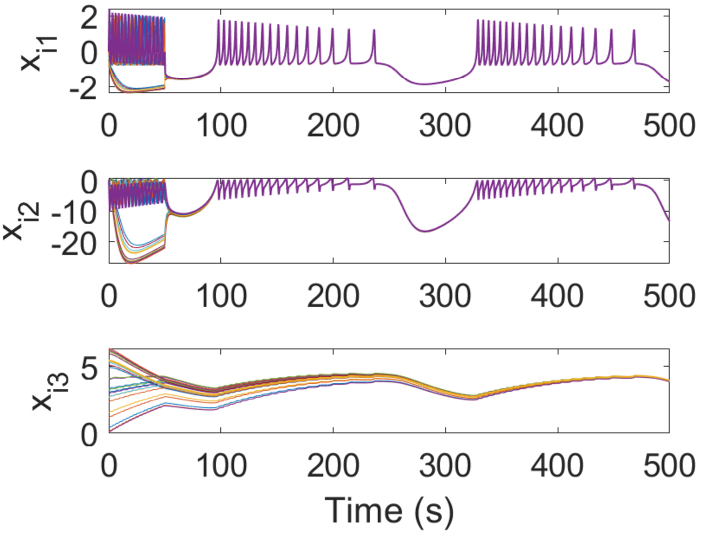

Figure 3: Dynamical behavior of the MNN states with memristive couplings where with $g_e = 8.0$ and $g_c = 2.5$.

by an electrical and memristive synapses (7)-(8). Where the chemical component is modeled as a memristor with a memristive function given by the sigmoidal function

$$\Gamma(\phi_{ij}(t)) = 1/[1 + exp^{-\lambda(u_{ij}(t)-\Theta_s)}] \tag{27}$$

with the parameters $\lambda = 10$, $\Theta_s = -0.25$ with $v_s = -2.0$ (that is inhibitory couplings [12]).

The numerical simulations for the results were performed using the ODE45 solver in MATLAB, which implements a fourth-order Runge–Kutta method with a variable time step, with an absolute tolerance (`AbsTol`) of 1×10^{-8} and a relative tolerance (`RelTol`) of 1×10^{-6}. In Figure 3 the simulation results of the numerical simulation of the MNN is shown. Initially the nodes are uncoupled ($g_e = g_c = 0$), then after $t = 200$ the neurons voltages $x_{1i}(t)$ are used to couple the neurons using ($g_e = 8.0$, $g_c = 2.5$) the dynamical behavior will converge to an identical synchronization; while the error between the neuron states (see Figure 4), converges to zero. Additionally, as expected the internal variables of the memristors in the chemical synapses go towards constant values as shown in Figure 4.

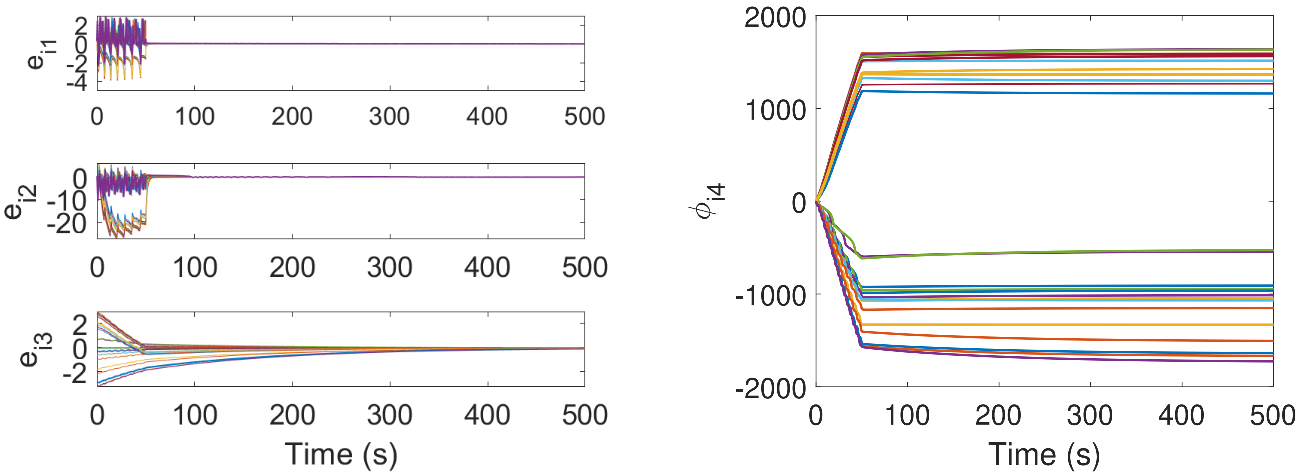

Figure 4: Errors of the MNN with $g_e = 8.0$ and $g_c = 2.5$ (left). Magnetic flux values of the memrisotrs (right).

The Lyapunov analysis in Equation (24) indicates that a sufficiently large g_e value is necessary to achieve synchronization, since the term $-g_e|\lambda_{2_A}|$ always contributes negatively to the error dynamics, promoting stability. However, the contribution of the chemical coupling (g_c) depends on the type of synapse.

Although inhibitory coupling ($v_s < 0$) was used in the simulations to obtain Figures 3-4, for which synchronization is strengthened by increasing g_c, in the case of excitatory synapses ($v_s > 0$) a value of g_c that is too large can destabilize synchronization. As shown in Figure 5, when g_c is very large, the neurons fail to synchronize, and their firing behaviors are affected, altering the shape of their peaks and bursts. However, for a sufficiently small value of g_c, the network synchronizes, although it was observed that the time required to achieve synchronization increases (see Figure 6).

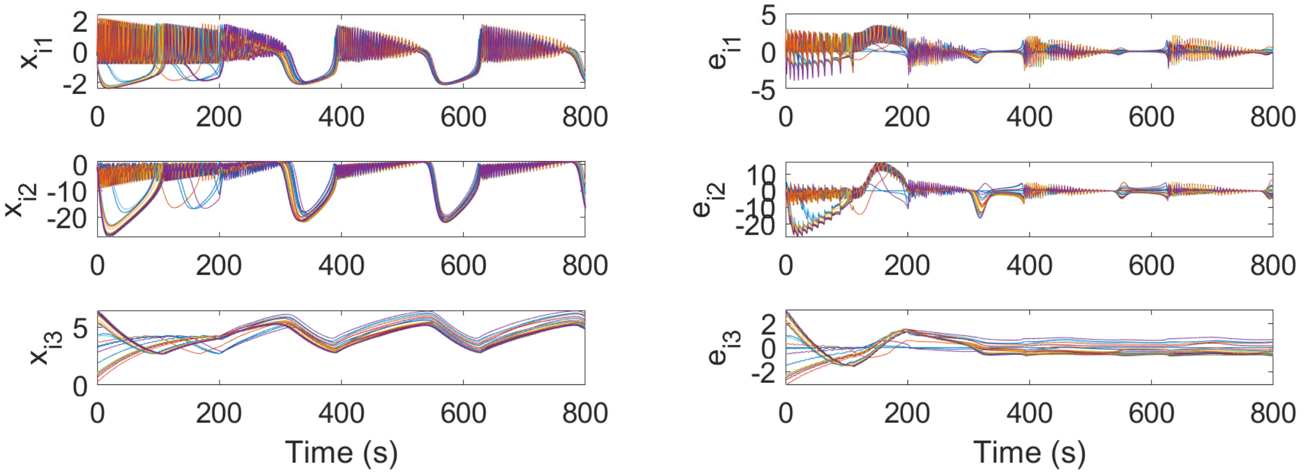

Figure 5: Dynamical behavior of the MNN states with inhibitory synapses and $g_e = 15$ and $g_c = 4$. (left). Errors of the MNN with inhibitory synapses(right).

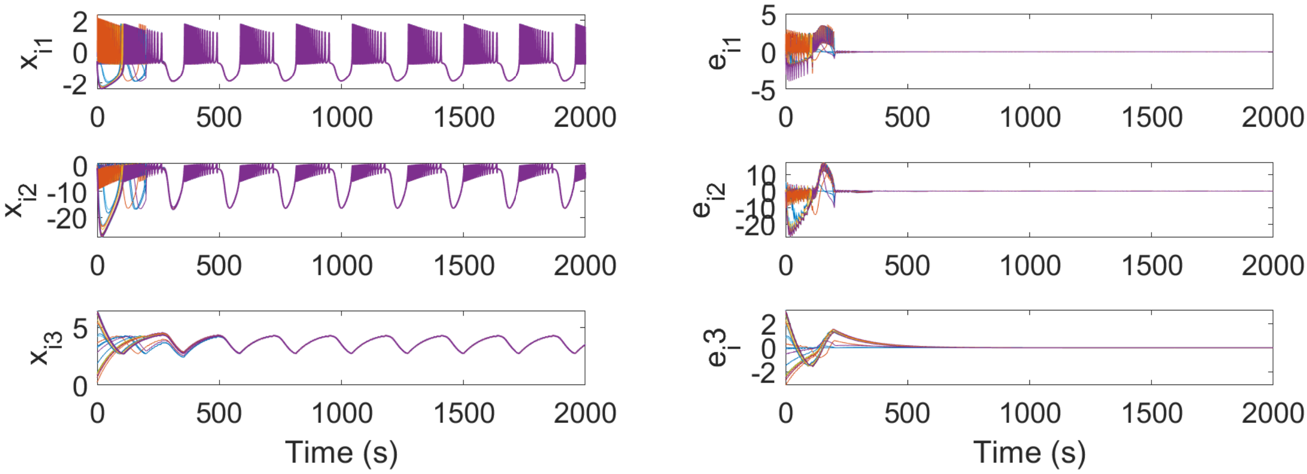

Figure 6: Dynamical behavior of the MNN states with inhibitory synapses and $g_e = 15$ and $g_c = 0.5$. (left). Errors of the MNN with inhibitory synapses (right).

5 Conclusion

In this study, we presented and analyzed a memristive neural network (MNN) composed of Hindmarsh-Rose (HR) neurons coupled by ideal memristors that function as chemical synapses. Our investigation established sufficient conditions for achieving identical synchronization within this network, with numerical simulations confirming the critical role of coupling strength in this process. The results show that for a sufficiently strong electrical coupling, synchronization is achieved, especially with inhibitory chemical couplings. A key observation is that when the network synchronizes, the internal variables (magnetic flux) of the memristors converge to a constant value, which demonstrates their ability to emulate important synaptic behaviors. We also confirmed that this identical synchronization can be achieved even in a complex network structure like a scale-free topology. These findings contribute to a deeper understanding of the relationship between memristor-based coupling and synchronization dynamics in neuromorphic engineering. While our model uses a sigmoidal memductance function due to its biological plausibility and mathematical properties, future work could explore the impact of other activation functions, such as hyperbolic tangent, piecewise-linear, or Morlet-type wavelets, on the network's dynamics and robustness. Extending the model to include stochastic inputs and delays, which are characteristic of real biological neurons, is also a crucial next step for assessing synchronization under more realistic conditions.

References

[1] M. I. Rabinovich et al. "Dynamical Principles In Neuroscience". In: *Reviews of Modern Physics* 78.4 (2006), pp. 1213–1265.

[2] E. M. Izhikevich. *Dynamical Systems in Neuroscience: The Geometry of Excitability and Bursting*. The MIT Press, 2007.

[3] F. Gabbiani and S. J. Cox. *Mathematics for Neuroscientists*. Academic Press, 2010.

[4] S. J. Russell and P. Norvig. *Artificial Intelligence: A Modern Approach*. Prentice-Hall Pearson, 2010.

[5] Y. Zhang et al. "Brain-inspired computing with memristors: Challenges in devices, circuits, and systems". In: *Applied Physics Reviews* 7.1 (2020), p. 011308.

[6] A. Adamatzky and L. O. Chua. *Memristor Networks*. Springer, 2014.

[7] L. O. Chua. "Memristor—The Missing Circuit Element". In: *IEEE Transactions on Circuit Theory* 18.5 (1971), pp. 507–519.

[8] L. O. Chua and S. M. Kang. "Memristive Devices and Systems". In: *Proceedings of the IEEE* 64.2 (1976), pp. 209–223.

[9] M. Pd. Sah et al. "Memristive Model of the Barnacle Giant Muscle Fibers". In: *International Journal of Bifurcation and Chaos* 26.1 (2016), p. 1630001.

[10] J. L. Hindmarsh and R. M. Rose. "A model of neuronal bursting using three coupled first order differential equations". In: *Proceedings of the Royal Society of London. Series B, Biological Sciences* 221.1222 (1984), pp. 87–102.

[11] M. Hua et al. "Memristive Single-Neuron Model and Its Memristor-Coupled Network: Homogenously Coexisting Attractors and Parallel-Offset Synchronization". In: *International Journal of Bifurcation and Chaos* 32.15 (2022), p. 2250225.

[12] M. S. Baptista, F. M. Moukam-Kakmeni, and C. Grebogi. "Combined effect of chemical and electrical synapses in Hindmarsh-Rose neural networks on synchronization and the rate of information". In: *Physical Review E* 82 (2010), p. 036203.

[13] X. F. Wang and G. Chen. "Synchronization in small-world dynamical networks". In: *International Journal of Bifurcation and Chaos* 12.1 (2002), pp. 187–192.

[14] C. H. Li and S. Y. Yang. "Eventual dissipativeness and synchronization of nonlinearly coupled dynamical network of Hindmarsh–Rose neurons". In: *Applied Mathematical Modelling* 39.21 (2015), pp. 6631–6644.